Konrad-Zuse-Zentrum
für Informationstechnik Berlin

Takustraße 7
D-14195 Berlin-Dahlem
Germany

PETER DEUFLHARD, MARTIN WEISER,
MARTIN SEEBASS[1]

A New Nonlinear Elliptic Multilevel FEM Applied to Regional Hyperthermia

[1]supported by Deutsche Forschungsgemeinschaft, Sonderforschungsbereich 273

Preprint SC 98-35 (December 1998)

A New Nonlinear Elliptic Multilevel FEM Applied to Regional Hyperthermia

Peter Deuflhard, Martin Weiser, Martin Seebaß

Konrad-Zuse-Zentrum für Informationstechnik Berlin
Takustr. 7, 14195 Berlin, Germany.
e-mail: {deuflhard,weiser,seebass}@zib.de

Abstract

In the clinical cancer therapy of regional hyperthermia nonlinear perfusion effects inside and outside the tumor seem to play a not negligible role. A stationary model of such effects leads to a nonlinear Helmholtz term within an elliptic boundary value problem. The present paper reports about the application of a recently designed adaptive multilevel FEM to this problem. For two 3D virtual patients, nonlinear and linear models are compared. Moreover, the numerical efficiency of the new algorithm is compared with a former application of an adaptive FEM to the corresponding instationary model PDE.

1 Introduction

Many stationary states of dynamic systems in biology, chemistry, physics and engineering are described by nonlinear elliptic PDEs. The solutions often have complex behavior and geometry, such that only adaptive methods are able to efficiently compute numerical solutions with required accuracy.

For linear elliptic PDE's, several adaptive multilevel FEM's are available — such as PLTMG [1], KASKADE [5], and UG [3, 4]. For nonlinear elliptic PDE's, both nonlinear MG [10] and linear MG algorithms [2, 8, 9] have been suggested. The present paper presents the extension of our hitherto 2D adaptive multilevel Newton FEM [8, 9] to 3D, in particular applied to the challenging therapy planning problem in regional hyperthermia [6, 7].

Hyperthermia, i. e. the local heating of tissue, is a recently developed method of cancer therapy, usually combined with radio- or chemotherapy. Electromagnetic waves to be absorbed are used as heat source.

2 Features of the Alogrithm

In this section we present a brief overview of our recently designed multilevel Newton method. For details and proofs, the reader may refer to [9].

2.1 Theoretical Background

Convex functional setting. The weak solution of a nonlinear elliptic PDE is the minimizer of the corresponding variational functional $f : D \subset X \to R$. Here, f is assumed to be a strictly convex C^2 functional defined on an open convex set D. In order to assure the existence of a minimum point $x^* \in D$, we assume that the real Banach space X is reflexive and that for some $x^0 \in D$ the level set $L_0 := \{x \in D \,|\, f(x) \leq f(x_0)\}$ is closed and bounded.

The nonlinear minimization problem is equivalent to the nonlinear operator equation

$$F(x) := f'(x) = 0, \quad x \in D, \tag{1}$$

that can be tackled by Newton's method. In order to guarantee the feasibility of Newton's method, we further assume that (1) is a strongly monotone problem. The ordinary Newton iteration is

$$\begin{aligned} F'(x^k)\Delta x_k &= -F(x^k) \\ x^{k+1} &= x^k + \Delta x_k \,. \end{aligned}$$

Since the Newton correction has to be approximated numerically by a finite element solution, we consider *inexact* Newton methods, wherein the Newton corrections Δx_k are approximated by inexact Newton corrections δx_k, leaving inner residuals r_k. Furthermore, damping is used for globalization. The global inexact Newton method now reads as

$$\begin{aligned} F'(x^k)\delta x_k &= -F(x^k) + r_k \\ x^{k+1} &= x^k + \lambda_k \delta x_k \,. \end{aligned}$$

Affine Conjugacy Invariance. In addition to the norm $||\cdot||$, we will be interested in local energy products defined by $\langle\cdot, F'(x)\cdot\rangle$. Motivated by the notation in Hilbert spaces, we write the induced norm shorthand as $\left\|F'(x)^{1/2}\cdot\right\|$.

Following [9], we want to carefully observe the associated affine conjugacy property, which means that we simultaneously treat the whole class of transformed convex minimization problems

$$g(y) = f(By) = \min\,, \quad x = By\,,$$

wherein B is understood to be an arbitrary isomorphism. By transformation, we arrive at the first and second derivatives

$$G(y) = B^* F(x)$$

and

$$G'(y) = B^* F'(x) B.$$

By construction, all G' are symmetric strictly positive operators. The associated linear system for the inexact Newton correction is

$$G'(y^k)\delta y_k = -G(y^k) + s_k \;\;\Leftrightarrow\;\; B^* F'(x^k) B \delta y_k = -B^* F(x^k) + s_k\,,$$

which implies $\delta x_k = \delta y_k$ as long as the inner iteration obeys the invariancy condition $s_k = B^* r_k$. It is therefore only natural to require affine conjugacy also for any damped Newton iteration both in the theoretical convergence analysis and in the algorithmic realization. As a consequence of such a requirement, any convergence theorems should only use affine conjugate theoretical quantities like functional values or local energy products.

Convergence results. To begin with, we are interested in the functional decrease obtained by the exact Newton method.

Theorem 2.1 *Let f be as defined above. Assume the special affine conjugate Lipschitz condition*

$$\left\|F'(x)^{-1/2}(F'(y) - F'(x))(y-x)\right\| \le \omega \left\|F'(x)^{1/2}(y-x)\right\|^2\,, \quad x, y \in D$$

holds for some $\omega < \infty$. For some iterate $x^k \in D$, define the quantities

$$\begin{aligned} \epsilon_k &:= \left\|F'(x^k)^{1/2}\Delta x^k\right\|^2 \\ h_k &:= \omega \left\|F'(x^k)^{1/2}\Delta x^k\right\|\,. \end{aligned}$$

Moreover, let $x^k + \lambda \Delta x_k \in D$ for $0 \le \lambda \le \lambda_{\max}$. Then

$$f(x^k + \lambda \Delta x^k) \le f(x^k) - t_k(\lambda)\epsilon_k \tag{2}$$

where $t_k(\lambda) = \lambda - \frac{\lambda^2}{2} - \frac{\lambda^3}{6} h_k$. The optimal choice of the damping factor is $\overline{\lambda}_k = \frac{2}{1+\sqrt{1+2h_k}} \le 1$.

From this theorem we may directly proceed to obtain the comparable results for the inexact Newton iteration. The inner iteration, which is formally represented by the introduction of the inner residual r_k, will be further specified to satisfy a Galerkin condition of the kind

$$\left\langle \delta x^k, F'(x^k)(\delta x^k - \Delta x^k) \right\rangle = \left\langle \delta x^k, r_k \right\rangle = 0$$

and to have a relative error denoted by

$$\delta_k := \frac{\left\| F'(x^k)^{1/2}(\Delta x^k - \delta x^k) \right\|}{\left\| F'(x^k)^{1/2} \delta x^k \right\|} .$$

For this specification, we immediately verify the following corollary:

Corollary 2.2 *The statements of Theorem 2.1 hold for inexact Newton-Galerkin methods as well, if only the exact Newton corrections Δx^k are replaced by the inexact Newton corrections δx^k and ϵ_k, h_k are replaced by*

$$\epsilon_k^\delta := \left\| F'(x^k)^{1/2} \delta x^k \right\|^2 = \frac{\epsilon_k}{1+\delta_k^2} , \; h_k^\delta := \omega \left\| F'(x^k)^{1/2} \delta x^k \right\| = \frac{h_k}{\sqrt{1+\delta_k^2}} .$$

With these local results established, we are now ready to formulate the associated global convergence theorem.

Theorem 2.3 *General assumptions as in Theorem 2.1 or Corollary 2.2, respectively (in the latter case δ_k bounded). Additionally, let F' be uniformly positive for all $x \in L_0$. Then the damped (inexact) Newton iteration with damping factors in the range $\lambda_k \in [\epsilon, \min(1, \lambda_k^{\max} - \epsilon)]$ and sufficiently small $\epsilon > 0$ depending on L_0 converges to the solution point x^*.*

2.2 Adaptive Strategies

The above theoretical results are the basis for the subsequent adaptive algorithmic strategies to determine the damping factor λ_k (in the outer loop) and the number of inner iterations.

Damping Strategy. We first construct a computational damping strategy on the basis of the theoretically optimal damping strategy as derived in the preceding section.

Therefore we replace the computationally unavailable Kantorovich quantities h_k by computational estimates $[h_k] \le h_k$ and the damping factors $\overline{\lambda}_k$ by $[\overline{\lambda}_k] := \frac{2}{1+\sqrt{1+2[h_k]}} \le 1$. Since $[h_k] \le h_k$, we have $[\overline{\lambda}_k] \ge \overline{\lambda}_k$ such that both a prediction strategey and a correction strategy need to be worked out. The efficiency of such a strategy will depend on the required accuracy of the computational estimate, which is analyzed in the following lemma.

Lemma 2.4 *Standard assumptions and notation as just introduced. Let*

$$0 \le h_k - [h_k] \le \sigma [h_k]$$

for some $\sigma < \infty$. Then, for $\lambda = [\overline{\lambda}_k]$, the following functional decrease is guaranteed:

$$f(x + \lambda \Delta x^k) \le f(x^k) - \left(\lambda - \frac{\lambda^2}{2} - \frac{\lambda^3}{3}(1+\sigma)(1-\lambda) \right) \tag{3}$$

If we require $\sigma \leq 1$, we arrive at the standard functional monotonicity test

$$f(x + \lambda \Delta x^k) \leq f(x^k) - \frac{\lambda}{6}(\lambda + 2)\epsilon_k \,,$$

if we further impose $\sigma \leq \frac{1}{2}$, i. e. if we require at least one exact binary digit in the Kantorovich quantity estimate, then (3) leads to the restricted monotonicity test

$$f(x + \lambda \Delta x^k) \leq f(x^k) - \frac{\lambda}{2}\epsilon_k \,.$$

As for the computational estimates $[h_k]$, we have three basic cheap ways of computational estimation which are based on functional, derivative and second derivative differences, respectively. We only present the functional based estimator here.

From inequality (2) we have the third order bound

$$E_3(\lambda) := f(x^k + \lambda \Delta x^k) - f(x^k) + \lambda \left(1 - \frac{\lambda}{2}\right) \epsilon_k \leq \frac{\lambda^3}{6} h_k \epsilon_k \,,$$

which, in turn, naturally inspires the computational estimate

$$[h_k](\lambda) := \frac{6|E_3(\lambda)|}{\lambda^3 \epsilon_k} \leq h_k$$

and leads to the correction strategy

$$\lambda_k^{i+1} := \frac{2}{1 + \sqrt{1 + 2[h_k](\lambda_k^i)}} \,.$$

In order to construct a theoretically backed initial estimate λ_k^0, we may recall that $h_{k+1} = \sqrt{\frac{\epsilon_{k+1}}{\epsilon_k}} h_k$ and define

$$[h_{k+1}]_0 := \sqrt{\frac{\epsilon_{k+1}}{\epsilon_k}} [h_k]_{i^*} \,,$$

where i^* denotes the index of the last computed estimate within the previous iterative step k. For $k \geq 0$, we are thus led to the prediction strategy

$$\lambda_{k+1}^0 := \frac{2}{1 + \sqrt{1 + 2[h_{k+1}]_0}} \leq 1 \,.$$

Still, the starting value λ_0^0 needs to be set ad hoc, taking into account the expected difficulty of the problem to be solved.

Accuracy Matching. With computational estimates for h_k^δ at hand, we now want to develop a suitable accuracy matching between the outer iteration (characterized by h_k) and the inner iteration (characterized by δ_k). Accuracy matching is a crucial aspect of multilevel Newton methods since the value of δ_k determines the character of the algorithm (from nonlinear multigrid to exact Banach space Newton method) as well as computing time.

A suitable criterion for choosing a specific accuracy matching is maximizing the information gain per unit work

$$i_k = \frac{I_k}{A_k}$$

within each step k. For global Newton methods, the information gain can be defined as

$$I_k := f(x^k) - f(x^{k+1}) \approx (1 + \delta_k^2)^{-\frac{3}{4}}.$$

Using adaptive linear finite element methods as inner iteration, the amount of work for step k can be estimated as

$$A_k \approx \delta_k^{-d}, \tag{4}$$

for δ_k small, where d is the spatial dimension. For the application to hyperthermia problems considered here, d equals 3 and we get

$$i_k \approx \frac{\delta_k^3}{(1 + \delta_k^2)^{3/4}},$$

which increases monotonically. Thus, choosing δ_k as large as possible seems to be preferable. On the other hand, (4) is only valid for δ_k small, and FEM error estimators are typically less reliable when the error is too large. Thus we suggest to choose δ_k moderately large, e. g. $\delta_k \approx 1$.

3 Application to Regional Hyperthermia

The above described algorithm has been recently applied to the challenging medical problem of therapy planning in regional hyperthermia.

3.1 Statement of the Mathematical Problem

Our model of heat transfer within the human body is Pennes' stationary bioheat-transfer equation (BHTE) [12]

$$\nabla(\kappa \nabla T) - cW\,(T - T_a) + \frac{1}{2}\sigma\,|E|^2 = 0$$

with the thermal conductivity κ, the blood perfusion W, the specific heat of blood c, the tissue temperature T and the temperature of arterial blood T_a. The source term $\frac{1}{2}\sigma\,|E|^2$, with electric conductivity σ, describes the absorbed power per volume of the electric field E. The electric field results from a superposition of four fields, generated by four antennas, which can be controlled separately in amplitude and phase. An optimization of these eight parameters is required for therapy in order to generate an optimal electric field.

Several experiments have shown that the response of vasculature in tissues to heat stress is strongly temperature-dependent [13]. When heated the blood flow in normal tissues, e. g. skin and muscle, increases significantly. In contrast, the tumor zone often appears to be so vulnerable to heat that the blood flow decreases upon heating. Taking this phenomenon into account results in a nonlinear Helmholtz term. Of course, the ellipticity of the equation depends on the function $W(T)$. Fortunately, for the actual functions derived from experimental data ellipticity is preserved in clinically reasonable temperature ranges. Since the directional second derivative $\langle v, F'(T)v\rangle$ comes out to be

$$\int_\Omega \kappa|\nabla v|^2 + (W'(T)(T - T_a) + W(T))v^2\,dx\,,$$

Tissue	Thermal Conductivity κ $W/m/^\circ C$	Electric Conductivity σ $1/m/\Omega$	Density ρ kg/m^3	Mass flow rate W $kg/s/m^3$
Fat	0.210	0.04	900	W_{fat}
Tumor	0.642	0.80	1000	W_{tumor}
Bladder	0.600	0.60	1000	5.000
Kidney	0.577	1.00	1000	66.670
Liver	0.640	0.60	1000	16.670
Muscle	0.642	0.80	1000	W_{muscle}
Bone	0.436	0.02	1600	0.540
Aorta	0.506	0.86	1000	83.330
Intestine	0.550	0.60	1000	3.333

Table 1: Material properties of tissues.

a *sufficient* condition for convexity is

$$W'(T)(T - T_a) + W(T) \geq 0. \tag{5}$$

This criterion, however, is not necessary because of the additional diffusion term $\kappa|\nabla v|^2$.

Boundary conditions are

$$\kappa \frac{\partial T}{\partial n} = h(T_{\text{out}} - T),$$

where T_{out} is the environmental temperature, and h is the heat transfer coefficient.

We use the same problem setting, especially the models of temperature-dependent blood perfusion in muscle, fat and tumor, as given in [11]:

$$\begin{aligned}
W_{\text{muscle}} &= \begin{cases} .45 + 3.55\exp(-(T-45)^2/12), & T \leq 45 \\ 4, & T > 45 \end{cases} \\
W_{\text{fat}} &= \begin{cases} .36 + .36\exp(-(T-45)^2/12), & T \leq 45 \\ .72 & T > 45 \end{cases} \\
W_{\text{tumor}} &= \begin{cases} .833, & T < 37 \\ .833 - (T-37)^{4.8}/5.438e3, & 37 \leq T \leq 42 \\ .416, & T > 42 \end{cases}
\end{aligned}$$

Although the perfusion model for tumor tissue fails to satisfy the convexity criterion (5) in the small temperature range from $41^\circ C$ to $42^\circ C$, the variational functional seems to be convex.

The remaining material constants are listed in table 1. For the linear model with constant perfusion we choose $W_{\text{fat}} = 0.54kg/s/m^3$, $W_{\text{muscle}} = 2.3kg/s/m^3$ and $W_{\text{tumor}} = 0.833kg/s/m^3$.

We further set $T_a = 37^\circ C$, $c = 3500Ws/kg/^\circ C$, $h = 45W/m^2/^\circ C$, and $T_{\text{out}} = 25^\circ C$.

3.2 Numerical Results

In order to study the effect of the temperature-dependent perfusion, we compare:

1. Computation with *linear* model, using antenna parameters derived from an optimization based on the linear model. This is the strategy currently used for therapy. The total power is adjusted such that normal tissue is not heated to more than $44°C$.

2. Computation with *nonlinear* model, using the same antenna parameters from optimizing the linear model. This result should be expected to show up in clinical therapy. Again, the total power is adjusted as above.

Cross-sections of the temperature field are shown in figures 1 and 2. The self-regulation of healthy tissue reflected by the nonlinear model reduces hot spots and thus permits a higher total power. This, together with the lower perfusion below $42°C$, leads to higher temperatures in large regions of the body and especially in the tumor. Temperature-volume histograms for tumor and muscle tissue are given in figure 3.

Throughout the computations, we compared our algorithm with KARDOS, a software package for solving timedependent PDE's, that has been applied to the same problems before. Care has to be taken in comparing such different methods in terms of efficiency, and therefore we restrict ourselves to some general remarks.

As expected, the stationary Newton multilevel approach outperforms the accurate time-dependent solution of the stationary BHTE clearly, thus providing a means for easier parameter studies for perfusion modelling as well as faster optimization of antenna parameters. On the other hand, the method is limited

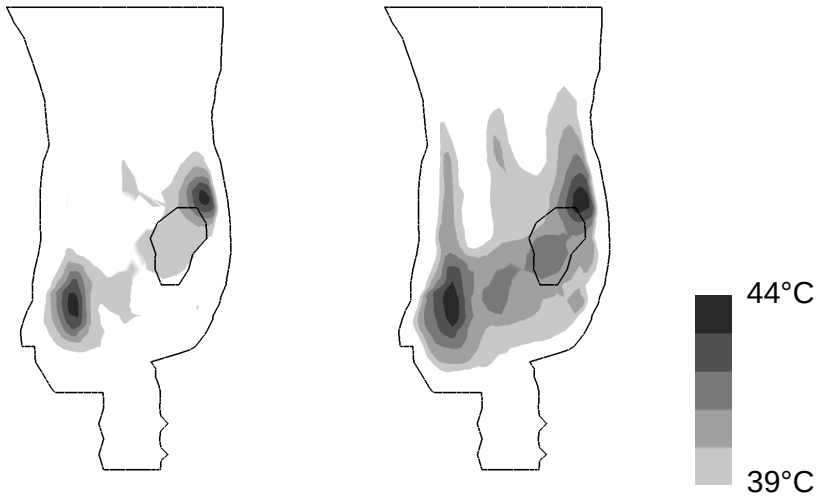

Figure 1: Temperature distribution in a cross-section of the pelvic region for virtual patient A. Results obtained with linear (left) and nonlinear model (right). Black lines: body outline and tumor contour.

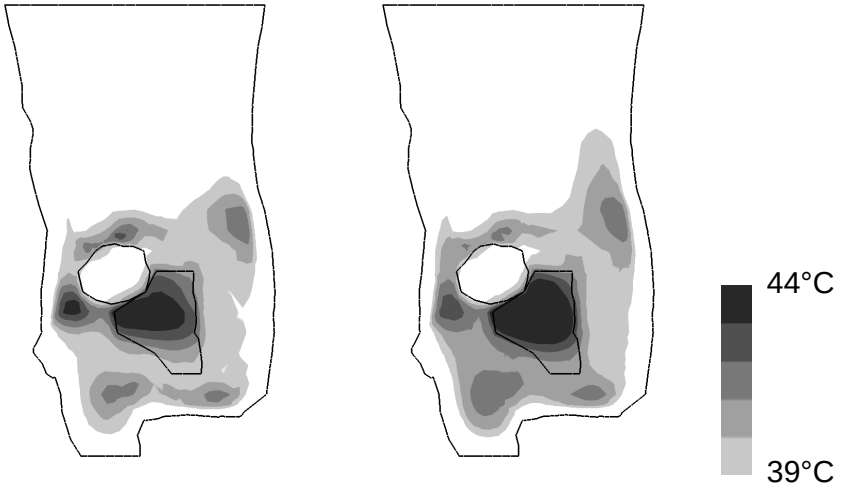

Figure 2: Temperature distribution in a cross-section of the pelvic region for virtual patient B. Results obtained with linear (left) and nonlinear model (right). Black lines: body outline, tumor and bladder contour.

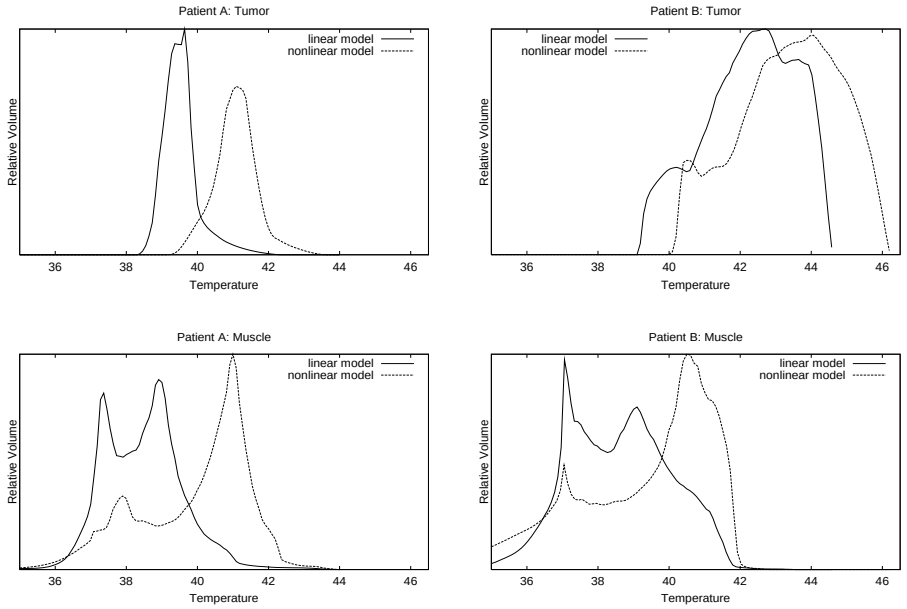

Figure 3: Temperature-volume histograms for tumor (top) and muscle (bottom). Patient A is shown on the left, patient B on the right.

to convex problems, thus limiting the modelling of the perfusion, and it does not provide any information about the transient phase of heating.

We emphasize the possibility of adopting the time-dependent method for stationary problems, thus leading to similar performance, but also to similar constraints on convexity and trajectory information.

4 Conclusions

The proposed algorithm is well applicable to challenging 3D problems and constitutes an efficient tool for stationary nonlinear hyperthermia problems. For two virtual patients, the linear and the nonlinear model were compared. The results suggest that the strategy currently used for therapy (i.e., optimization based on the linear model) is a conservative one, since the predictions of the linear model are more pessimistic in terms of tumor heating. This finding should be checked for more patient models. Furthermore, optimization based on the nonlinear model should be considered, where even better results can be expected.

Acknowledgement The authors wish to thank P. Wust from Virchow-Klinikum Berlin for his inspiring cooperation and support, and B. Erdmann for his help in comparing NEWTON-KASKADE with KARDOS.

References

[1] R. E. Bank. *PLTMG: A Software Package for Solving Elliptic Partial Differential Equations. User's Guide 8.0.* SIAM, Philadelphia, 1998.

[2] R. E. Bank and D. J. Rose. Analysis of a multilevel iterative method for nonlinear finite element equations. *Math. Comput.*, 39:453–465, 1982.

[3] P. Bastian, K. Birken, K. Johannsen, S. Lang, N. Neuss, H. Rentz-Reichert, and C. Wieners. UG – A Flexible Software Toolbox for Solving Partial Differential Equations. *Computing and Visualization in Science*, (to appear).

[4] P. Bastian and G. Wittum. Adaptive multigrid methods: The UG concept. In W. Hackbusch et al, editor, *Adaptive methods - algorithms, theory and applications. Proceedings of the 9th GAMM-Seminar Kiel, Germany, January 22-24, 1993*, volume 46 of *Notes Numer. Fluid Mech.*, pages 17–37, Braunschweig, 1994. Vieweg.

[5] R. Beck, B. Erdmann, and R. Roitzsch. Kaskade 3.0, an object-oriented adaptive finite element code. Technical Report 95-4, ZIB, 1995.

[6] P. Deuflhard and M. Seebaß. Adaptive Multilevel FEM as Decisive Tools in the Clinical Cancer Therapy Hyperthermia. Preprint SC 98-30, ZIB, 1998.

[7] P. Deuflhard, M. Seebaß, D. Stalling, R. Beck, and H.-C. Hege. Hyperthermia Treatment Planning in Clinical Cancer Therapy: Modelling, Simulation and Visualization. In A. Sydow, editor, *Proc. of the 15th IMACS World Congress 1997 on Scientific Computation: Modelling and Applied Mathematics*, volume 3, pages 9–17. Wissenschaft und Technik Verlag, 1997.

[8] P. Deuflhard and M. Weiser. Local inexact Newton multilevel FEM for nonlinear elliptic problems. In M.-O. Bristeau, G. Etgen, W. Fitzigibbon, J.-L. Lions, J. Periaux, and M. Wheeler, editors, *Computational science for the 21st century*, pages 129–138. Wiley, 1997.

[9] P. Deuflhard and M. Weiser. Global inexact Newton multilevel FEM for nonlinear elliptic problems. In W. Hackbusch and G. Wittum, editors, *Multigrid Methods V*, Lecture Notes in Computational Science and Engineering, pages 71–89. Springer, 1998.

[10] W. Hackbusch and A. Reusken. Analysis of a damped nonlinear multilevel method. *Numer. Math.*, 55(2):225–246, 1989.

[11] J. Lang, B. Erdmann, and M. Seebaß. Impact of Nonlinear Heat Transfer on Temperature Control in Regional Hyperthermia. Preprint SC 97-73, ZIB, 1997.

[12] H. H. Pennes. Analysis of tissue and arterial blood temperatures in the resting human forearm. *J. Appl. Phys.*, 1:93–122, 1948.

[13] C. W. Song, A. Lokshina, J. G. Rhee, M. Patten, and S. H. Levitt. Implication of blood flow in hyperthermic treatment of tumors. *IEEE Trans. Biomed. Engrg.*, 31:9–16, 1984.